Global Journal of Science Frontier Research: a
Physics and Space Science
Volume 20 Issue 8 Version 1.0 Year 2020
Type : Double Blind Peer Reviewed International Research Journal
Publisher: Global Journals
Online ISSN: 2249-4626 & Print ISSN: 0975-5896

Effects of Indium Composition and the Size on the Electronic Structure Ns-Np of Quantum Dots in N/$In_xga_{1-X}n$/Ligand

By F. Benhaddou, H. Abboudi, I. Zorkani, A. Jorio & S. J. Edrissi

Sidi Mohammed Ben Abdellah University

Abstract- The electronic structure of homogeneous and inhomogeneous quantum dots involves fascinating optoelectronic properties. Herein, a detailed theoretical and numerical investigation of the electronic structure of spherical inhomogeneous quantum dots InN/$In_xGa_{1-x}N$/Ligand, based Indium and Gallium Nitride, with a variable composition x of Indium. A more real profile is adopted with a finite potential shell and variable thickness. The ligand and solution impose external confinement. With such shell $In_xGa_{1-x}N$, a minimum of defects is ensured at the interface, and the structure is passivated. Along with this work, we will explore the effects of the various parameters of this nanosystem on its gap, on the location of charge carriers and the distribution of nS-nP energy levels. We will show how the dimensions of the material core InN, the material shell $In_xGa_{1-x}N$, and the Indium-composition x control the characteristics of the nanosystem and consequently improve the electronic and optical properties. Then a detailed calculation of the electronic structure will be made.

Keywords: inhomogeneous quantum dot; core/shell; electronic structure; two levels system; quantum efficiency; photostability.

GJSFR-A Classification: FOR Code: 020699

Strictly as per the compliance and regulations of:

Effects of Indium Composition and the Size on the Electronic Structure Ns-Np of Quantum Dots in $N/In_xga_{1-X}n/Ligand$

F. Benhaddou [α], H. Abboudi [σ], I. Zorkani [ρ], A. Jorio [ω] & S. J. Edrissi [¥]

Abstract- The electronic structure of homogeneous and inhomogeneous quantum dots involves fascinating optoelectronic properties. Herein, a detailed theoretical and numerical investigation of the electronic structure of spherical inhomogeneous quantum dots $InN/In_xGa_{1-x}N/Ligand$, based Indium and Gallium Nitride, with a variable composition x of Indium. A more real profile is adopted with a finite potential shell and variable thickness. The ligand and solution impose external confinement. With such shell $In_xGa_{1-x}N$, a minimum of defects is ensured at the interface, and the structure is passivated. Along with this work, we will explore the effects of the various parameters of this nanosystem on its gap, on the location of charge carriers and the distribution of nS-nP energy levels. We will show how the dimensions of the material core InN, the material shell $In_xGa_{1-x}N$, and the Indium-composition x control the characteristics of the nanosystem and consequently improve the electronic and optical properties. Then a detailed calculation of the electronic structure will be made.

Keywords: inhomogeneous quantum dot; core/shell; electronic structure; two levels system; quantum efficiency; photostability.

I. Introduction

Since the 80s,[1-4] the advent of nanotechnology and the development of growth techniques quantum dots has advanced a lot in favor of the development of optoelectronic components, [5-10] light-emitting diodes,[11] biological applications,[12] photovoltaic[13] and quantum information.[14] These nanostructures have remarkable properties, especially the quantum confinement of the charge carriers, which induces a total discretization of their energy levels. Luminescence is their strongest point but far from being the only one. They are thus emitters of single photons and even at room temperature. Also, around 1990, when these nanostructures were enveloped by shells[15,16] to form a quantum dot core/shells system ; these properties became fascinating. In today's scientific field, quantum dots take up an important place and greatly attract the curiosity and interest of researchers. We obtain the sources of light with a very fine spectrum, photo-stables, and with excellent quantum efficiency.[17,18] They are controlled by size and shape.[19-24] To remedy the defects still presented by these nanostructures such as the blinking[25] and to functionalize them in various environments for multiple applications, growth design has improved by adsorption of ligands covering the outer shell. The hetero-nanosystems thus obtained core/shell/Ligand[25,26] would become true light emitters.[27] These properties essentially arise from the electronic structure they possess. Many structures based on II-VI or III-V semiconductor core have already been analyzed and studied as CdSe, HgS, ZnS, and CdS.[5][28] In parallel, other materials are also currently attracting researchers such as indium nitride and gallium nitride.[29,30] This current work is a theoretical investigation of the characteristics of colloidal quantum dots $InN/In_xGa_{1-x}N/Ligand$. We will focus our study on the calculation of the electronic structure of levels nS-nP and the effects of the composition and size on their electronic and optical properties. We want to say how we can control these

Author α σ ρ ω ¥: Group of Nanomaterials and Renewable Energy, Sidi Mohammed Ben Abdellah University, Faculty of Sciences, LPS, Dhar Lmahraz 30000, BP. 1796, Fez, Morocco.
e-mail: farid.benhaddou@laposte.net

characteristics and how to make it capable of improving the fascinating properties of homogeneous quantum.

II. Model and Formalism

The study of quantum dots core/shell has aroused the interest of researchers for their important properties. In those studies, various geometric confinement models have adopted. The current investigation, the confinement of shell is modeled by a continuous and finite potential while that imposed by the colloidal solution, and the ligand is infinite. The graphic 1 is a schematic representation of potential with the values calculated in the case where the composition of indium $x = 0.3$. The height of the barrier for the electron is at 1.672eV and at -0.469eV for the hole. The bottom of the gap is taken as the origin of the potentials.

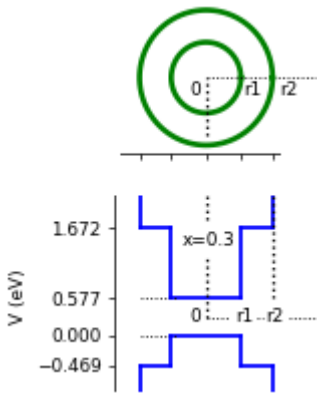

Figure 1: Schematic representation of QD and potential profile for indium composition $x = 0.3$

In the isotropic, nondegenerate parabolic approximations and under effective mass approach the energy E and envelope wave function $\Psi(\vec{r})$ of the electron or hole are determined by solving the eigenvalues equation in spherical coordinates of Hamiltonian :

$$H\Psi(\vec{r}) = E\Psi(\vec{r}) \quad \text{with} \quad H = (\frac{\hbar}{i}\nabla)\frac{1}{2m^*}(\frac{\hbar}{i}\nabla) + \mathrm{V}(r) \tag{1}$$

The envelop wave function is expressed by the form $\Psi_{n\ell}(\vec{r}) = R_{n\ell}(r)Y_\ell^m(\theta,\varphi)$, where $Y_\ell^m(\theta,\varphi)$ is the spherical harmonic. $R_{n\ell}(r)$ radial components and the integer numbers n,ℓ,m check the values : $n = 1,2,3.....$ $\ell = 0,1,2.....$ $m = 0,\pm1,\pm2,.....,\pm\ell$. The potential $\mathrm{V}(r)$ and effective mass are respectively given by :

$$\mathrm{V}(r) = \begin{cases} 0 & 0 < r \le r_1 \\ \mathrm{V}_0^{e,h}(x,T) & r_1 \le r \le r_2 \\ \infty & r \ge r_2 \end{cases} \qquad m^*(r) = \begin{cases} m^*(\mathrm{InN}) & 0 < r \le r_1 \\ m^*(\mathrm{In}_x\mathrm{Ga}_{1-x}\mathrm{N}) & r_1 \le r \le r_2 \end{cases} \tag{2}$$

For solving the equation (1) of eigenvalues and in our following calculations, we will use the average mass between InN material and $In_xGa_{1-x}N$ alloy. To use the effective mass of alloy.[31]

$$m^*_{e,h}(In_xGa_{1-x}N) = xm^*_{e,h}(InN) + (1-x)m^*_{e,h}(GaN)$$

Rearrange with the values of parameters in table 1 to give :

$$\overline{m}^*_e / m_0 = -0.0700x + 0.1200 \quad (3)$$

$$\overline{m}^*_h / m_0 = -0.0175x + 0.8225 \quad (4)$$

Denoted later m^*_e / m_0 and m^*_h / m_0. The confinment potential $V_0^{e,h}(x,T)$ is function of indium composition x and temperature T according:[32.33]

$$V_0^{e,h}(x,T) = h_{e,h}(E_g(In_xGa_{1-x}N,T) - E_g^{InN}(T))$$

by substitution[34] of $E_g(In_xGa_{1-x}N,T) = xE_g^{InN}(T) + (1-x)E_g^{GaN}(T)$. we get

$$V_0^{e,h}(x,T) = h_{e,h}((1-x)(E_g^{GaN}(T) - E_g^{InN}(T)) - bx(1-x))$$

Where $h_e = 0.7$; $b = 1.43eV$ are respevtivly the rate of electronic confinement and bowing parameter[35-37] and $h_h = 1 - h_e$.

Let $$E_g^{GaN}(T) = E_g^{GaN}(0) - (0.593/(600+T)).10^{-3}.T^2$$

$$E_g^{InN}(T) = E_g^{InN}(0) - (0.245/(624+T)).10^{-3}.T^2$$

And introdicing the follow temperature[32] parameter.

$$f = \left(0.593/(600+T) - 0.245/(624+T)\right).10^{-3}.T^2$$

Giving: $$V_0^{e,h} = h_{e,h}\left[(1-x)\Delta E_g(0) + (x-1)f - bx(1-x)\right] \quad (5)$$

Denoted later V_0, where $\Delta E_g(0) = E_g^{GaN}(0) - E_g^{InN}(0)$ calculated using the values given in table 1. Modifying the temperature from 0K to 300K, V_0 varies slightly, therefore the temperature has no marked effect on the confinement of this nanostructure and our calculations will be at 300K temperature. However, when the indium composition increases, V_0 decreases, and the confinement decreases all the more for the holes.

Table 1: The characteristic parameters of InN and GaN.[38]

Parameters	GaN	InN
$E_g(0)$ (eV)	3.3	0.6
m^*_e / m_0	0.19	0.054
m^*_h / m_0	0.81	0.835
ε_∞	5.75	8.4

In this spherical symmetry we use spherical cordinates so the equation (1) becomes :

$$-\frac{1}{r}\frac{\partial^2}{\partial r^2}(rR_n^{\ell}(r)) + \left[\frac{\ell(\ell+1)\hbar^2}{r^2} + \frac{2m^*}{\hbar^2}(V(r)-E)\right]R_n^{\ell}(r) = 0$$

We are interested after that in bound states such that the energy E verifies $E < V_0$. According to this our above main equation becomes :

$$-\frac{1}{r}\frac{\partial^2}{\partial r^2}(rR_{n\ell}(r)) + \left[\frac{\ell(\ell+1)}{r^2} - k^2\right]R_{n\ell}(r) = 0 \qquad 0 < r \le r_1 \quad (6)$$

$$-\frac{1}{r}\frac{\partial^2}{\partial r^2}(rR_{n\ell}(r)) + \left[\frac{\ell(\ell+1)}{r^2} + K^2\right]R_{n\ell}(r) = 0 \qquad r_1 \le r \le r_2 \quad (7)$$

Where $k^2 = \frac{2m^*E}{\hbar^2}$; $K^2 = \frac{2m^*(V_0 - E)}{\hbar^2}$ and $K^2 = k_0^2 - k^2$

Above relations constitute two forms of the generating equation of Bessel functions. To solve these equations we proceed to change variables from r to $\rho = kr$ for the first equation, from r to $\rho = iKr$ for the second and by using the function $Z = \rho^{1/2} R_{n\ell}(r)$ instead $R_{n\ell}(r)$. If replaced into the above equations the solution is :

$$\rho^{-1/2} Z(\rho) = \begin{cases} \mathrm{C}_1.(kr)^{-1/2} J_{\ell+1/2}(kr) + \mathrm{D}_1.(kr)^{-1/2} Y_{\ell+1/2}(kr) & 0 < r \le r_1 \\ \mathrm{A}_1.(iKr)^{-1/2} I_{\ell+1/2}(Kr) + \mathrm{B}_1.(iKr)^{-1/2} K_{\ell+1/2}(Kr) & r_1 \le r \le r_2 \end{cases} \quad (8)$$

$\mathrm{A}_1, \mathrm{B}_1$, C_1 and D_1 are constants. $J_{\ell+1/2}$ and $Y_{\ell+1/2}$ are the classical Bessel functions, respectively of the first and second kind. $Y_{\ell+1/2}$ is infinite at the origin, so the constant D_1 must have a null value. $I_{\ell+1/2}$ and $K_{\ell+1/2}$ are the modified or hyperbolic Bessel functions of the first and second kind. These functions are designed to give a real solution. In our case, we will use the spherical Bessel functions $j_\ell(kr)$ and spherical Hankel functions $h_\ell^{(1)}(iKr)$ of the first kind, which is more suitable and simple with spherical symmetry. Therefore the solution is :

$$R_{n\ell}(r) = \begin{cases} \mathrm{C}_1\sqrt{2/\pi}.j_\ell(kr) & 0 < r \le r_1 \\ \mathrm{A}_1\sqrt{2/\pi}.e^{-i\ell\pi/2}.j_\ell(iKr) + \mathrm{B}_1\sqrt{\pi/2}.e^{i\ell\pi/4}.h_\ell^{(1)}(iKr) & r_1 \le r \le r_2 \end{cases}$$

Simplify this $$R_{n\ell}(r) = \begin{cases} \mathrm{C}.j_\ell(kr) & 0 < r \le r_1 \\ \mathrm{A}e^{-i\ell\pi/2} j_\ell(iKr) + \mathrm{B}e^{i\ell\pi/4} h_\ell^{(1)}(iKr) & r_1 \le r \le r_2 \end{cases} \quad (9)$$

Where $\mathrm{C} = \mathrm{A}_1.\sqrt{2/\pi}$; $\mathrm{A} = \mathrm{A}_1.\sqrt{2/\pi}$ and $\mathrm{B} = \mathrm{B}_1.\sqrt{2/\pi}$.

We focus at this step of determining the wave functions and energies for the nS and nP states. At this point, by applying the matching condition of $R_{n0}(r)$ in r_2 we can express $\mathrm{B} = -\beta.(\mathrm{A}/2)$ where $\beta = 1 - e^{2Kr_2}$. Knowing that $j_0(\rho) = \sin(\rho)/\rho$ and $h_0^{(1)}(iKr) = -(1/Kr)e^{-Kr}$ the relation (8) gives the wavefunction for nS states

$$R_{n0}(r) = \begin{cases} \mathrm{C}\dfrac{\sin(kr)}{kr} & 0 < r \le r_1 \\ \mathrm{A}\left[\dfrac{1}{2Kr}(e^{-Kr} - e^{Kr}) - \beta\dfrac{e^{-Kr}}{2Kr}\right] & r_1 \le r \le r_2 \end{cases} \quad (10)$$

Furthermore by applying the conditions of continuity to the wavefunction in r_1 we obtain the expression of C as a function of A and after normalization we can calculate numerically A for fixed values of the composition x, the radius r_1 and the thickness $\Delta = r_2 - r_1$.

Employing the matching conditions for the wavefunction which give the following system :

$$\begin{cases} \mathrm{C}\dfrac{\sin(kr_1)}{kr_1} = \mathrm{A}\left(\dfrac{e^{-Kr_1} - e^{Kr_1}}{2Kr_1} - \beta\dfrac{e^{-Kr_1}}{2Kr_1}\right) \\ \mathrm{C}k\left(\dfrac{\cos(kr_1)}{kr_1} - \dfrac{\sin(kr_1)}{(kr_1)^2}\right) = \mathrm{A}K\left(\dfrac{e^{Kr_1} - e^{-Kr_1}}{2(Kr_1)^2} - \dfrac{e^{Kr_1} + e^{-Kr_1}}{2Kr_1} + \beta\dfrac{e^{-Kr_1}}{2(Kr_1)^2} + \beta\dfrac{e^{-Kr_1}}{2Kr_1}\right) \end{cases}$$

Canceling the determinant of this system it follows

$$\frac{\tan(kr_1)}{kr_1} = \frac{1}{Kr_1}\frac{1 - e^{2K(r_2 - r_1)}}{1 + e^{2K(r_2 - r_1)}} \quad (11)$$

Rearrange to give a quantification function $Q^{\mathrm{S}}_{\eta,r_2,k,x}(\mathrm{X})$ with a reduced variable X :

$$Q^{\mathrm{S}}_{\eta,r_2,k,x}(\mathrm{X}) = \frac{\tan(\alpha\mathrm{X})}{\alpha\mathrm{X}} - \frac{1}{\alpha\mathrm{Y}}\frac{1 - \exp(2\alpha\mathrm{Y}\Delta r/r_1)}{1 + \exp(2\alpha\mathrm{Y}\Delta r/r_1)} \quad (12)$$

Where $\alpha = k_0 r_1$. $X = kr_1 / \alpha$. $\Delta r = r_2 - r_1$ and $Y = Kr_1 / \alpha = \sqrt{1 - X^2}$

Let's do the same for the nP states. We use the matching condition of wavefunction for $r = r_2$ we can express $B = -\beta.(A/2)$ where $\beta = 1 + ((Kr_2 - 1)/(Kr_2 + 1))\exp(2Kr_2)$. We replace the following items $j_1(kr) = (\sin(kr)/(kr)^2) - (\cos(kr)/kr)$ and $h_1^{(1)}(iKr) = i((1/Kr) + (1/(Kr)^2)\exp(-Kr)$ in relation (9) wich becomes :

$$R_{n1}(r) = \begin{cases} C\left(\frac{\sin(kr)}{(kr)^2} - \frac{\cos(kr)}{kr}\right) & 0 < r \le r_1 \\ A\left[\left(\frac{1}{2(Kr)^2}(e^{-Kr} - e^{Kr}) + \frac{1}{2Kr}(e^{-Kr} + e^{Kr})\right) - \beta\left(\frac{1}{Kr} + \frac{1}{(Kr)^2}\right)e^{-Kr}\right] & r_1 \le r \le r_2 \end{cases} \quad (13)$$

The conditions of continuity to the wavefunction for $r = r_1$ give the expression of C as a function of A and, the normalization condition allows us to calculate A for each (x . r_1 r_2). In this case too, using the same calculation methods with the same variable we have :

$$\frac{1}{\alpha X \tan(\alpha X)} - \frac{1}{(\alpha X)^2} = \left(\frac{1}{\alpha Y} + \frac{1}{(\alpha Y)^2}\right)\omega(r_1, r_2, Y)$$

Where $$\omega(r_1, r_2, Y) = \frac{((\alpha Y r_2 / r_1 - 1)/(\alpha Y r_2 / r + 1)) - (\alpha Y - 1)/(\alpha Y + 1)e^{-2\alpha Y(r_2 - r_1)/r_1}}{((\alpha Y r_2 / r_1 - 1)/(\alpha Y r_2 / r + 1)) + e^{-2\alpha Y(r_2 - r_1)/r_1}}$$

Therefore the quantification is determined by $Q^P_{r_1, r_2, k, x}(X)$:

$$Q^P_{r_1, r_2, k, x}(X) = \frac{1}{\alpha X \tan(\alpha X)} - \frac{1}{(\alpha X)^2} - \left(\frac{1}{\alpha Y} + \frac{1}{(\alpha Y)^2}\right)\omega(r_1, r_2, Y) \quad (14)$$

The energies of the nS-nP states are given by the zeros of the quantization functions $Q^S_{r_1, r_2, k, x}(X)$ and $Q^P_{r_1, r_2, k, x}(X)$ gived by the expressions (12) and (14). But these functions cancel each other out if $\alpha X \rangle \frac{\pi}{2}$. That is to say :

$$X \rangle X_0(x, r1) = \pi\hbar^2 / 4m^* V_0 r \quad (15)$$

$X_0(x, r1)$ is increasing as fuction of the composition x according to the relation (4) but in reverse for core radius r_1. This condition constitutes a limit not to be exceeded for geometric confinement.

To study the distribution of the nS levels, we have established a function $F(E_{ns})$ which depends on the energy. For this, we have reformulated the equation (12) to give the relation :

$$F(E_{nS}) = \frac{\sin(kr_1)}{kr_1}.Kr_1.\frac{1 + \exp(-2K\Delta r)}{1 - \exp(-K\Delta r)} = \cos(Kr_1) \quad (16)$$

So $$-1 \le F(E_{ns}) \le +1$$

This function is limited and its graphic study, in figure 4, shows that the nS energies of the states are distributed according to disjoint allowed mini-bands AMB.

To give credibility to the physical context of our calculations, we are going to consider boundary behavior. The quantum dot with an infinite barrier is obtained when r_2 tends to infinity. Let's tend r_2 to infinity in the equation (11). the term

$(1-\exp(2K(r_2-r_1))/(1+\exp(2K(r_2-r_1))$ converges to -1. The equation is reduced to $\tan(kr_1)/kr_1=-1/Kr_1$. This is the relation effectively governing a quantum dot in continuous potential model.[28] When $r_1 \to r_2$ this term tends to 0, so $\tan(kr_1)=0$ relation describing a quantum dot in infinite potential model. In the same way of nS-states, we will explore the behavior of nP-states at the limits. When $r_2 \to +\infty$ then $\exp(-K(r_2-r_1)) \to 0$ so $\omega \to 1$ and we find the result of the quantum dot in the finite potential for nP states characterized by the equation $(\cot an(kr)/kr)\text{-}(1/(kr)^2)=1/Kr+1/(Kr)^2$. When $r_1 \to r_2$ $\omega \to 0$. the equation (13) is reduced to $\tan(kr_1)/kr_1=1/kr_1$. This is the same behavior that has been observed with the quantum dot in the infinite potential model[27].

III. Result and Discussion

As previously established, the wavefunction for nS states is given by the expression in relation (9). For a total radius $r_2=10$ nm and three values of Indium-composition $x=0$; 0.3 ; 0.6 we study the wavefunction of fundamental electronic state 1S and the associated radial probability over the entire nanostructure as function of the radius r of the quantum dot. The results are shown in graphics 2.a, 2.b, 3.a and 3.b. Figures 2 represent the wave functions of the electron and the hole in their ground states, and the figures 3 represent their radial probability of presence. Note that for a smaller radius $r_1=3$ nm, the particles are partially localized in shell, especially for the holes where the confinement is weaker. They are localized for a large radius core $r_1=7$ nm even if x varies from 0 to 0.6. This partial delocalization is considered as a defect for the photostability[5][17,18][25] and the quantum efficiency[5][17,18] of colloidal quantum dots core/shell type. The partial delocalization in the shell causes a spectral red shift[17] of the luminescence and it causes an increase in the times of de-excitation of the electron-hole pairs by radiative or non-radiative recombination.[25][39-41] We can see that with a core radius of the order of a few nanometers ensuring sufficient but not excessive confinement and with a thicker shell, the nanostructure ensures the location of electron-hole pairs in the core material.

An experimental study by P. Reiss et al. has shown that the growth of a fairly large layer of the shell improves photostability[5][17,18] and quantum efficency[5][17,18][25]. We notice then that the theoretical results above move in the same direction. They agree with this experimental study and show the crucial role of localization in this improvement. Other studies have highlighted the same conclusions.[19][41,42] Therefore the choice of the core radius, the shell-thickness and, the Indium-composition control the localization of the particles in the core material. The advantage of the shell is then to reinforce the confinement and to passivate the structure and consequently to improve the optical properties.

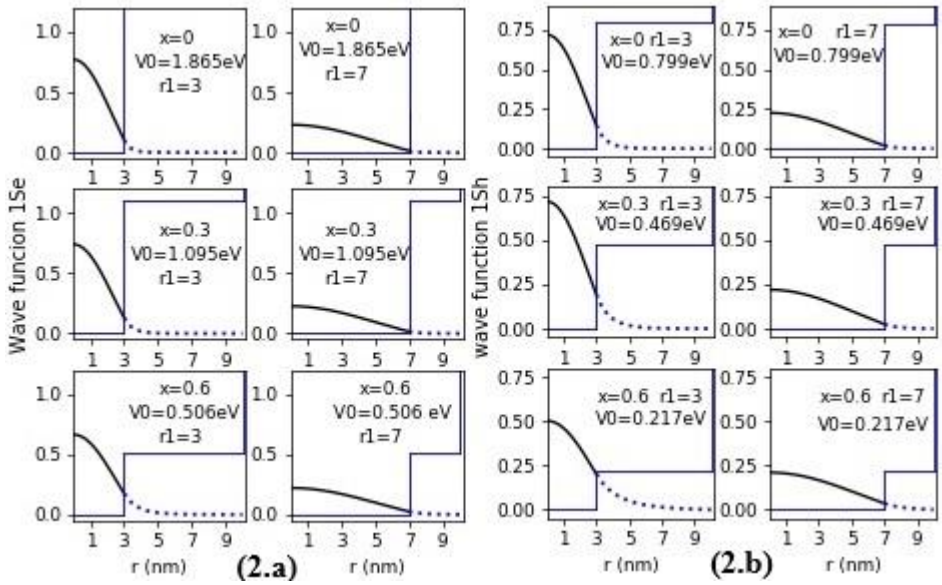

Figure 2: Continuous and dotted curves radius *r* dependent wave function of the ground state for various values of composition *x*, core radius r_1 and potential V_0. Blue square lines represent the potential. (2.a) electronic states (2.b) hole states

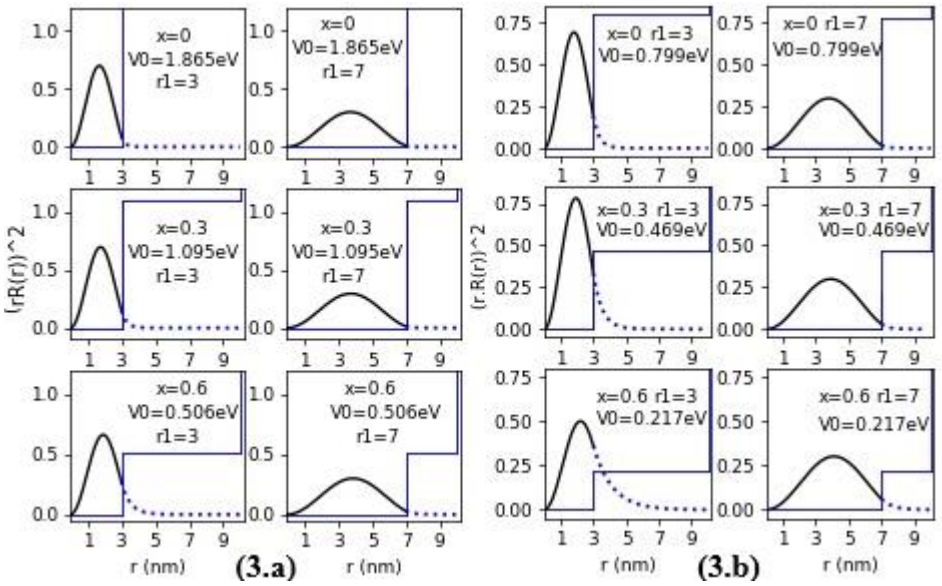

Figure 3: Curves in continuous or dotted lines represent the electronic radial probability in ground state vs radius *r* for various values of composition *x*, core radius r_1 and, potential V_0. Blue square lines represent the potential. (3.a) electronic states (3.b) hole states

About the distribution of nS levels. The graphical study of the relation (16) gives the figure 4. For each value of the trio (x, r_1, r_2), the energies $E_{nS} = E_{1s}, E_{2s}, E_{3s}.....$ of the nS states are included in possible allowed mini-bands AMB. But only a few levels that can be authorized and occupied in these bands. The energies of these levels have been calculated and will be given in the following part. These mini-bands are separated by mini-gaps MG. Figure 4 shows the existence of these AMB and MG. These curves represent the

function $F(E_{nS})$ given by expression (16) for the electron and hole with two values of indium composition.

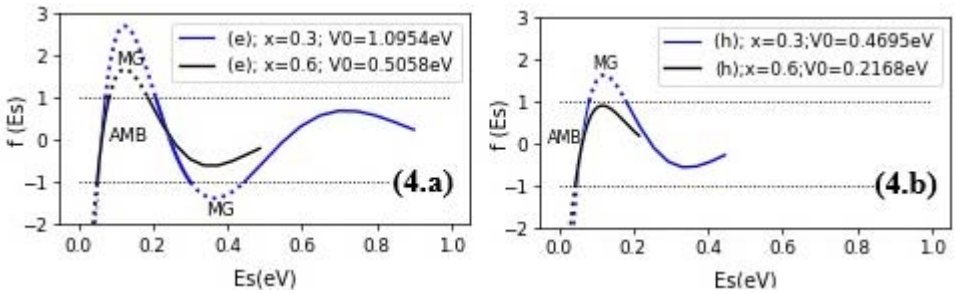

Figure 4: Showing curves of AMB and MG (4.a) for electron for the values x =0.3; 0.6. (4.b) for hole for the values x =0.3; 0.6.

For energies of nS and nP states, the formalism above, the numerical and graphical study of the zeros of the functions $Q^{S}_{r_1,r_2,k,x}(X)$ and $Q^{P}_{r_1,r_2,k,x}(X)$ defined in the expresions (12) and (14) give the quantification and allow the calculation repectivly of the energies E_{nS} of nS states and E_{nP} of nP states :

$$E_{nS} = \frac{\hbar^2 k_{nS}^2}{2m^*} = \frac{\hbar^2 k_0^2 X_{nS}^2}{2m^*} = V_0 X_{nS}^2 \quad (17)$$

$$E_{nP} = \frac{\hbar^2 k_{nP}^2}{2m^*} = \frac{\hbar^2 k_0^2 X_{nP}^2}{2m^*} = V_0 X_{nP}^2 \quad (18)$$

The table 2 lists the values found of E_{nS} and E_{nP}, by varying the composition x for $r_1 = 7\text{nm}$ and $r_2 = 10\text{nm}$. Note that these values respect the order observed in the atom or in a homogeneous quantum dot [27].

Table 2: Values of energy of nS and nP levels versus composition x for $r_1 = 7\text{nm}$. $r_2 = 10\text{nm}$. $T = 300K$.

x	E1s	E1p	E2s	E2p	E3s	E3p	E4s	E4p	E5s
0	0.0569	0.1164	0.2273	0.3209	0.5098	0.6259	0.9009	1.1242	1.3921
0.1	0.0597	0.1220	0.2381	0.3593	0.5332	0.7113	0.9392	1.1687	1.4375
0.2	0.0626	0.1279	0.2495	0.3763	0.5573	0.7422	0.9760	1.2064	
0.3	0.0657	0.1342	0.2615	0.3937	0.5815	0.7714	1.0050		
0.4	0.0689	0.1407	0.2735	0.4109	0.6035	0.7942			
0.5	0.0722	0.1472	0.2849	0.4262	0.6189				
0.6	0.0752	0.1530	0.2941	0.4365					
0.7	0.0775	0.1572	0.2989						
0.8	0.0785	0.1585							
0.9	0.0775								

Regarding the effect of various parameters on the energy of the ground state. The curves of figure 5 show the evolution of the 1S energy state calculated as a function of the indium composition, the radius of core and, thickness of the shell. We note in figure 4 the strong effect of confinement with the small sizes.[25][27][43] Indeed, the electronic energy of the ground state increases when the radius of the core material decreases. We notice the

existence of maximums indexed on the curves by signs (+). The impact of the composition x is only felt for the low values of r_1. For a large value of x and a small value of r_1 there is no electronic bound state. Fixed size, the composition has only a slight effect on the ground state. Its effect is especially marked for the number of bound states and for higher levels.

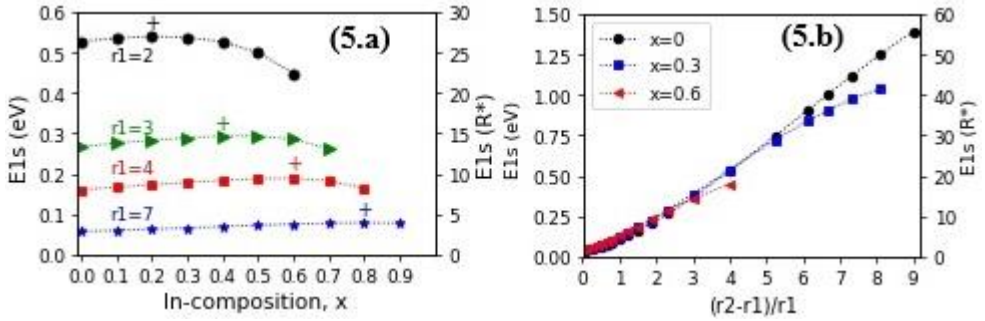

Figure 5: (5.a) Indium composition dependent energy E_{nS} for various values of r_1.
(5.b) Variation of E_{nS} vs $\Delta r / r_1$ for various values of x.

In table 2, and figure 5, for a structure with a total radius $r_2 = 10\text{nm}$, a core radius $r_1 = 7\text{nm}$ and indium composition $x = 0.9$, we obtain a two-level system 1Sh-1Se. Even for a Indium-composition value of 0.8 or 0.7, the difference $E_{1P} - E_{1S}$ is significant and the fundamentatl states 1Se and 1Sh are isolated. Our structure is equivalent to a two-level system characterizing the structure to be photostable and temporally coherent[27][44-46]. Indeed by resonant excitation 1Sh-1Se, we obtain a system where the only radiative emission is via the transition 1Se-1Sh and consequently the time of de-excitation 1Se-1Sh and the time between two successive photon emissions doe not change. This property is essential for the design of coherent light sources as Laser.

The quantum dots colloid core/shell are widely used as luminescent sources as light-emitting diodes, lasers, or as biological probes. Our system gives us optical control by radius core r_1 and thickness of shell $\Delta r = r_2 - r_1$. The gap can be varied in a wide spectral range. It has been shown in figures 6.a and 6.b that the effective band gap can be incraesed from 0.6391eV to 1.5319eV. For total radius $r_2 = 10$ nm of the nanostructure, we note that the gap increases by decreasing the radius of core material, or by increasing the thickness of shell. It is the effect of confinement in all nanostructures. Recall that by controlling the effective band gap we can choose the fundamental emission frequency.

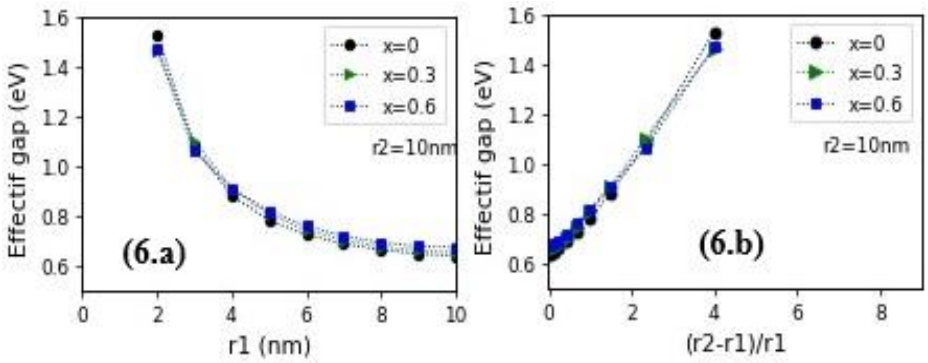

Figure 6: (6.a) Core radius dependent effect if gap. For various values of composition x.
(6.b) Thickness of shell dependent effectif gap. For various values of composition x.

Another time, figure 6 confirms what has been shown in the previous paragraph that the composition x has no marked effect on the gap or the ground state. The energies of the hole states have also been calculated. Below in the figure 7 we represent the electronic structure nS-nP of the inhomogeneous quantum dots InN/In$_x$Ga$_{1-x}$N/Ligand. The origin of the energies is taken on the height of the valence band. Only a few levels of the previously described nS energy bands AMB constitute possible levels. The nP levels can be found in the mentioned mini gaps MG and represented in figure 6. By comparing two structures with compositions 0.3 and 0.6 we notice that the number of bound states nS or nP decreases when x increases. The manipulation of the size and the Indium-composition allows the control of electronic structure design and consequently allows the control of electronic and optical properties of the nanostructure.

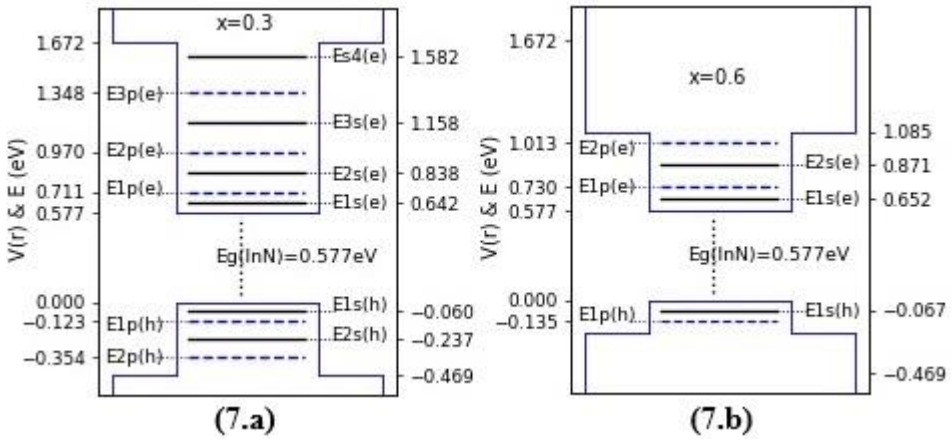

Figure 7: Electronic structure nS and nP for $InN / In_xGa_{1-x}N$ / Ligand for the values $x = 0.3;\ 0.6$ of indium composition and $T = 300K$

IV. Conclusion

Analytical and numerical methods were used to obtain electronic structure nS-nP of inhomogeneous quantum dots InN/InxGa1-xN/Ligand. The nanostructure allows a triple optoelectronic control. A wide range of gaps is allowed. The calculations show that a large value of core-radius, a small value of shell-thickness and a low value of Indium-composition, involve the localization of particles in the core material. This result reinforces the photostability and the qauntum efficiency of the nanostructure. These optical properties are essential for the realization of many devices such as light sources, detectors, biological markers. We conclude that in addition to the properties of the homogeneous quantum dot, the inhomogeneous quantum dot studied allows the electronic and optical control by shell thickness, and by Indium-composition. The presence of the shell improves the optical properties and the Indium-composition marks the design and the number of levels in the electronic structure. We can obtain a two levels system. This last result offers the condition of temporal coherence required to produce temporally coherent light sources such as a laser.

References Références Referencias

1. L. E. Brus. (1983) *J. Chem.Phys.*, 79, 5566.921.
2. Brus. L.E. & al. (1984) *Chem. Phys*., 80(9), 4403-4409.
3. A. L. Efros & al. (1996) *Phys. Rev.* B., 54, 4843.
4. A.I. Ekimov. A.A. Onushchenko. (1981) *Sov. JETP. Lett.*, 34, 345.

5. A. R. AbouElhamd. (2019) *Eneriges*., 12, 1058.
6. E. Finkman & al. *(*2000) *Physica E.*, (1-2), 139-45.
7. H.C. Liu & al. (2001) *Applied Physics Letters,* 78(1), 79-81.
8. Coe S & al. (2002) *Nature,* 420, 800.
9. Robel I. & al. (2006) *J. Am. Chem. Soc.* 128(7), 2385-93
10. A. V. Malko & al. *(*2002) *Appl. Phys. Lett.* 81, 1303.
11. C. Ruan & al. (2016) *Nanomaterials*. 6, 13.
12. D. Gao & al. (2014) *Adv. Funct. Mater.*, 24, 3897–3905.
13. C. Yuan & al. (2016) *Nanomaterials* 6, 97.
14. M. D. Shulman & al. (2012) *Science.* 336, 6078, pp. 202-205.
15. A. Eychmuller. A. Mews. H. Weller, (1993) *Chem. Phys. Lett*., 208. 59–62.
16. J.Th.G. Overbeek*, J.W. Goodwin.* (1982) *The Royal Society of Chemistry,* London*.*
17. P. Reiss, M. Protiere, and Liang Li, (2009),Core/Shell Semiconductor Nanocrystals, I*nterscience small*, 5, No. 2, 154–168.
18. Reiss, P.; Bleuse, J. Pron, A., (2002), Highly Luminescent CdSe/ZnSe Core/Shell Nanocrystals of Low Size Dispersion, *Nano Lett.*, 2(7), 781-784.
19. Talapin. D. V. & al. *Nano Lett*.(2001), 1(4), 207-211.
20. W.W. Yu & al. (2003) *Chem. Mater*. 15, 2854-2860.
21. De Melle Donega & al. (2003) *Journal of physical chemistry B,* 107(2), 489-496.
22. Qu. L. & al. (2002) *Am. Chem. Soc.*, 124. 2049-2055.
23. Sapra & al. (2006) *Journal of Materials Chemistry*, 16(33). 3391-3395.
24. Song & al. (2010) *Chemical Communications*, 46(27). 4971-4973.
25. B. Mahler & al. (2008) *Nat. Mater.* 7, 659.
26. A. P. Alivisatos (2004) *Nat. Biotechnol.* 22, 47.
27. F. Benhaddou & al. (2015) *Physica B*, 477, 100–104.
28. J. W. Haus & al. (1993) *Physical Review B.* 47(3), 1359.
29. Junie H. & al. (2019) *Scientific reports*, 9. 12048.
30. Injamam U. I. C. & al. *(*2018) *Results in Physics*, 9, 432-439.
31. J. Mycielsky and A. M. Witowski. (1986) *Phys. Stat. Sol.* (b), 134, 675.
32. Y. P. Varshni. (1967) *Physica,* 1(34), 149–154.
33. I. Vurgftman. J. R. Meyer. *(*2003) *J. Appl. Phys.* 94(6), 3675–3696.
34. J. A. Van Vechten and T. K. Bergstresser. (1970) *Phys. Rev. B1*., 3351.
35. D. Richardson. 1972 *J. Phys.: Solid Stat. Phys.* 5L27.
36. A. N. Pikhtin, F.T. Poluprovodn, (1977) *Sov. Phys. Semicond.*, 11, 245.
37. O. Madelung. (1964) Phys of III-V compounds, Wiley and Sons, New-York , , 269, 139-40.
38. P. Rinke & al. (2008) *Phys. Rev. B*, 77, 075202–075215.
39. A. L. Efros and M. Rose (1997) *Phys. Rev. Lett.*, 78(6), 1110-1113.
40. P. Spinicelli et al. (2009) *Phys. Rev. Lett.*, 102, 136801.
41. W. van Roosbroeck. W. Shockley. (1954) *Phys. Rev.*, 94, 1558-1560.
42. S. Bull & al. (2009) *Journal of Physics B.*, 42, 114003 (pp).
43. F. Benhaddou & al. (2017) *AIP Advences,* 7. 065112.
44. A. Zrenner et al., (2002), Coherent properties of a two-level system based on a quantum-dot photodiode. *Nature* 418, 612–614.
45. T. Faust, J. Rieger, M.J. Seitner, J.P. Kotthaus and E.M. Weiq, (2013), Coherent control of a classical nanomechanical two-level system, *Nature Physics* v. 9, p485–488.
46. X.Wu & al, (2003) *Nature Biotechnol.,* 21 (4), 41-46.

Data Availability

The data that supports the findings of this study are available within the article or from the corresponding author upon reasonable request.